

Dwarf galaxy merger-induced star formation rate: A case study of Mrk 1481

Daya Nidhi Chhatkuli^{1,*}, Sanjaya Paudel², Amrit Sedain³
Binil Aryal⁴

¹Tri-Chandra Multiple Campus, Tribhuvan University, Kathmandu, Nepal

²Department of Astronomy, Yonsei University, Seoul 03722, Republic of Korea

³Institut für Physik und Astronomie, Universität, Potsdam, Karl-Liebknecht-Str. 24/25,
14476 Golm, Germany

⁴Office of Institute of Science and Technology, Tribhuvan University
Kathmandu, Nepal

*Corresponding author. Email: chhatkulidn@gmail.com

Abstract

The merger of the galaxies serves as a trigger for the increase in the galaxy's star formation rate (SFR), which can be quantified by observing the column density of the H α line. Our findings report the presence of various gas and metal emission lines, strongly indicating that the galaxy hosts very young stars and is currently undergoing active star formation processes. Notably, we report a relatively high SFR of $\sim 0.0055 M_{\odot} \text{ yr}^{-1}$ for a dwarf galaxy, alongside a metallicity level of $12 + \log(O/H) \sim 8.88$ dex. Our photometric analysis reinforces the notion that the galaxy is in the midst of a merger phase. Additionally, the analysis indicates that the galaxy has a relatively flat shape (Sérsic index ~ 0.8), with stars distributed more broadly and less concentrated toward its center. This provides further evidence of the ongoing merger and its impact on the galaxy's structure. The half-light radius of the galaxy is estimated to be 2.73 arcsec by using the Petrosian method.

Keywords

Dwarf Galaxy, Galaxy Merger, Star Formation Rate, Galaxy Morphology.

Article information

Manuscript received: November 30, 2023; Revised: January 16, 2024; Accepted: January 24, 2024

DOI <https://doi.org/10.3126/bibechana.v21i2.60334>

This work is licensed under the Creative Commons CC BY-NC License. <https://creativecommons.org/licenses/by-nc/4.0/>

1 Introduction

Galaxies are captivating celestial entities, offering a window into the cosmos. Their study provides valuable insights into the origins and dispersion of elements and energy, shedding light on the enigmatic

forces of dark matter and dark energy shaping the universe [1–3]. Galaxy mergers represent a crucial aspect of galactic evolution, wherein two or more galaxies combine, resulting in a single, larger entity. These mergers engender interactions among stars,

gas, dust, and dark matter, leading to the redistribution and reconfiguration of the newly formed galaxy's components. Spanning millions to billions of years, these processes exert a profound influence on the structure, star formation history, and evolution of the resultant galaxy. Additionally, galaxy mergers can trigger intense starbursts and are associated with the formation of some of the universe's most massive galaxies. These mergers primarily occur due to gravitational forces, giving rise to major mergers between comparably sized large galaxies, minor mergers where smaller galaxies are absorbed by larger ones, cannibal mergers where a smaller galaxy is absorbed by a larger one, and tidal mergers where galactic tidal forces pull stars together. Dry galaxy mergers, specifically involving galaxies with limited gas and dust, often lead to the creation of elliptical or spiral galaxies, depending on the galaxies involved, playing a pivotal role in reshaping galactic structures and features, even when their gas and dust reservoirs are depleted [4–6]. Studying dwarf-dwarf galaxy mergers is important because dwarf galaxies were common in the early universe and drove galaxy mergers. Yet, these mergers are often too far away to see directly, and finding low-redshift ones with dual active galactic nuclei (DAGN) is tough. In a recent study, scientists found the first two DAGN candidates in these mergers, known for their telltale tidal signs and dual, bright X-ray sources, likely linked to actively feeding massive black holes. More research will give us valuable insights into how galaxies grew early on, how black holes formed in their centers, and how mergers triggered star formation [7–9].

The star formation rate (SFR) measures the rate at which new stars form, driven by the gravitational collapse of interstellar gas and dust into protostars and stars. Various factors influence SFR, including interstellar medium density, composition, temperature, and nearby stars. Methods for SFR measurement include observations of star-forming regions, infrared surveys, and calculations based on region mass and star formation time. SFR plays a pivotal role in galaxy evolution, star distribution, and understanding galaxy formation. In galaxy mergers, SFR can significantly rise due to increased gravitational potential, compressing gas and dust and redistributing them, fostering higher star formation. Studying SFR during mergers offers insights into how these events influence star formation dynamics and galaxy evolution, with a notable connection to metallicity, as higher metallicity enhances gas cooling efficiency, promoting increased SFR, while lower metallicity can suppress it, as observed in galaxies such as the Milky Way [10–13].

Merging galaxies exhibit elevated metallicity levels compared to normal galaxies because the gas in mergers, which is abundant, gets transformed

into stars, enriching the galaxy with metals. This heightened metal abundance results from the substantial star and gas content in merging galaxies. Moreover, metals in merging galaxies can redistribute to other galaxies, further boosting their metallicity [8, 14–16].

Galaxy morphology is a fundamental field in astronomy that explores the shapes and structures of galaxies. It enables us to uncover the secrets of how galaxies form and evolve, providing valuable insights into the broader structure of the universe. One of the major advantages of galaxy morphology is the ability to understand the various life stages of the galaxy's evolution and the influence of external factors such as mergers [17, 18]. The surface brightness profile of a galaxy, essential for understanding its structure and components like the bulge, disk, and halo, is typically determined by analyzing the distribution of light from stars and gas. The Sérsic profile, a mathematical model, is developed by Miguel A. Sérsic, quantifies this brightness distribution, aiding in galaxy shape characterization via the Sérsic index (n) – low n values suggest diffuse galaxies, while high n values indicate concentrated ones. The profile helps distinguish galaxy types, such as ellipticals and spirals, determine galaxy size (effective radius), and estimate total luminosity for mass calculations. To understand the complex dynamics and morphology of interacting dwarf galaxy, we can employ a double Sérsic profile model [19].

Here, we present the study of the morphology of a merging dwarf galaxy, Mrk 1481, and calculate its SFR by using the flux of the emission line of the galaxy spectrum. Moreover, we estimate the size and Sérsic index of the galaxy.

2 Material and Methods

2.1 Sample Selection

Interacting dwarf galaxies present fascinating opportunities for the study of their photometric characteristics. In our investigation, we focused on a tidally interacting dwarf galaxy, Mrk 1481, of low redshift ($z = 0.0059$) with a radial velocity of 1803 km s⁻¹ selected from the catalog by Paudel et. al, 2018 [20]. The apparent g and r -band magnitudes of the galaxy are 16.48 mag and 15.87 mag respectively. Its absolute B-band magnitude is -15.49 mag. It has a stellar mass of $2.2 \times 10^8 M_{\odot}$. This specific galaxy, Mrk 1481, is situated at celestial coordinates R. A. (J2000): 13^h 42^m 59.4^s and Dec. (J2000): 52° 41' 17.88". We determined its distance to be approximately 25.03 Mpc, calculated from its redshift, assuming a flat universe and adopting cosmological parameters ($H_0 = 71$ km s⁻¹ Mpc⁻¹, $\Omega_m = 0.3$, and $\Omega_{\Lambda} = 0.7$). The number of neighbors within the search criteria (sky-projected distance

of fewer than 700 kpc and a relative line-of-sight radial velocity of less than ± 700 km/s) is 9, and it has no satellite. Notably, the mass ratio between the interacting dwarf galaxies M_1 and M_2 is 20. The SDSS optical image and its spectrum are shown in **Figure 1**. In the image, the blue part repre-

sents the area where stars are currently forming in the galaxy. This is mainly happening because of the gravitational pull between the two dwarf galaxies, which causes them to interact. The spectrum shows strong emission lines, which indicates that the galaxy is an emission type.

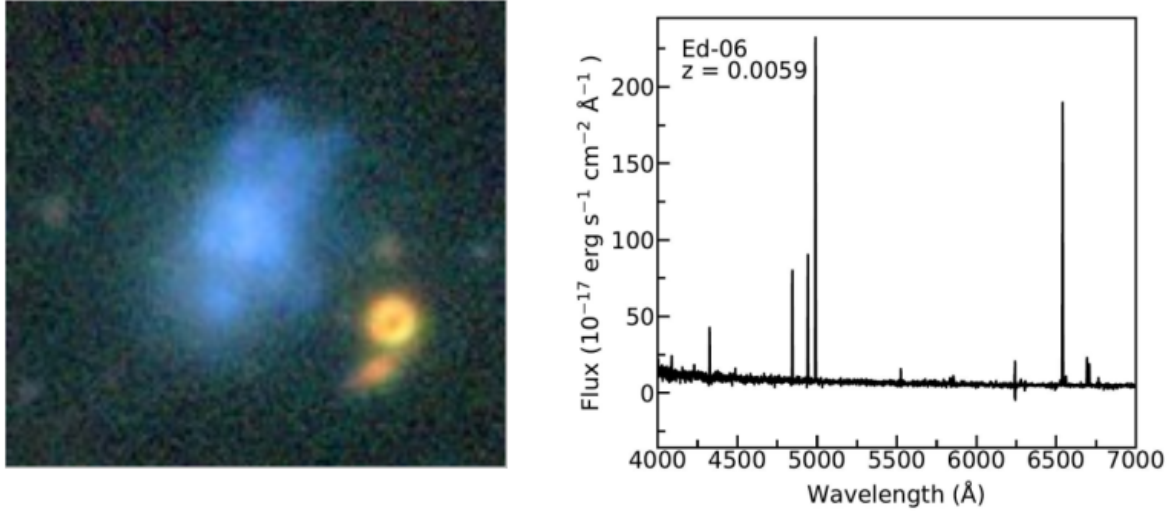


Figure 1: The SDSS optical image of the emission-type interacting dwarf galaxy Mrk 1481 is shown in the left panel and its optical spectrum is shown in the right panel. The X-axis is the rest-frame wavelength and Y-axis is flux.

2.2 Data Analysis

We examine the gas content of the galaxy by analyzing its optical spectrum obtained from the SDSS Data Archive Server (DAS). Our analysis aims to understand the galaxy's composition. It is important to note that we relied on archival data and didn't apply any additional data processing to the galaxy's spectra. To reproduce the spectra from the SDSS data server, we utilize a tool called TOPCAT. The SDSS fiber, which collects this data, has a diameter of 3 arcsecs, covering only a small portion of the galaxy. The SDSS optical spectrum ranges from 4,000 Å to 7,000 Å, encompassing key emission and absorption lines often used to study the chemical properties of stars and galaxies.

We used a Gaussian fit analysis to examine the prominent emission lines in the spectra, revealing a combination of hydrogen and metal lines within the galaxy. To calculate the galaxy's star-formation rate, we applied the Kennicutt initial mass function and used neutral hydrogen's luminosity. This approach is based on [21, 22]. We took a closer look at the way the interacting galaxy appears in pictures to figure out where its tidal effects come from. The major axis light profile of the galaxy is extracted by using the Image Reduction and Analysis Facility (IRAF) task ellipse, and the best-fitted elliptical isophotes are drawn on the image as described by

Jedrzejewski [23]. To estimate the galaxy's size, we applied the Sérsic profile [24], which helps us understand how big the galaxy is. We also used Photutils to see how the galaxy's shape changes over time. This helped us getting a better idea of what the galaxy looks like by studying its brightness patterns in images. We obtained the g-band image of the galaxy from the SDSS data server and employed IRAF to generate the fitted image of the galaxy using the Sérsic profile. In the following section, we will delve into the outcomes of our analysis.

3 Results and Discussion

3.1 Spectroscopic Analysis

In our study, we focused on analyzing the galaxy's key emission lines, including H_β , $OIII_{5008}$, H_α and NII_{6585} , (see **Figure 2**). Black dots correspond to the observed flux, while the red solid lines depict the Gaussian fit applied to the galaxy's data. These lines are significant for assessing the SFR and gaining insights into the galaxy's metallicity. The major cause of the broadening of the characteristic lines is Doppler's broadening.

The Balmer decrement is the ratio of the fluxes in the H_α and H_β lines often used to estimate the amount of dust along the line of sight. The Balmer decrement is used in astronomy to measure the red-

dening and attenuation of light from astronomical objects, particularly in the study of galaxies and nebulae. The Balmer decrement is also used to determine the dependence of the Balmer decrement with galaxy stellar mass and to study the evolution of the Balmer decrement with redshift [25]. We calculated the value of Balmer increment to be 3.15. In the context of a merging dwarf galaxy, a Balmer decrement of 3.15 indicates a significant amount of dust, which affects the observed colors and spectra of the galaxy. This value suggests that the light from the galaxy is being heavily scattered and absorbed by dust, impacting the interpretation of its properties and the processes occurring within it [26–28].

The galaxy’s star formation rate determined from the neutral hydrogen line before extinction correction stands at $0.0046 \text{ M}_{\odot}\text{yr}^{-1}$. The SFR is significantly influenced by the presence of dust particles in the interstellar medium, particularly impacting the H_{α} emission, where a substantial amount is absorbed. To address this, we calculated the galaxy’s extinction coefficient, which is measured to be 0.1997. It’s worth noting that the H_{β} line is less affected by dust particle interaction. Consequently, after correcting for extinction, the SFR of the galaxy is $0.0055 \text{ M}_{\odot}\text{yr}^{-1}$ which is almost similar to the Zhao et al. [29], where they calculated star formation as $0.0058 \text{ M}_{\odot}\text{yr}^{-1}$ and after the extinction correction, $0.0339 \text{ M}_{\odot}\text{yr}^{-1}$. This high value of SFR of this galaxy indicates that the galaxy is actively forming stars at a significant rate. The high SFR can lead to the formation of massive stars, which can then die in supernova explosions and enrich the surrounding environment with heavy elements [30]. For the full calculation of the star formation rate and the extinction correction, see [7].

We also determined the metallicity ratios for some of the prominent lines, providing insights into the galaxy’s evolution and characteristics. Gas-phase metallicity is commonly assessed by calculating the oxygen abundance relative to hydrogen, defined as $12 + \log(\text{O}/\text{H})$. This is due to oxygen’s significance in both the mass of the universe and the electron temperature of the gas. In our analysis, we found that the metallicity of our interacting dwarf galaxy stands at 8.86 dex [31] (calculated as 8.69 dex). This suggests that the galaxy’s outer regions have become hotter because the ionizing photons have been absorbed by the metals, impacting their properties. A high value of metallicity means that

the galaxy contains a significant number of heavy elements, such as iron, in its stellar population [32].

3.2 Photometric Analysis

In our study, we employed Photutils to analyze the galaxy’s isophotes and their orientation, as depicted in the upper left panel of **Figure 3**. The evident twisting in these isophotes strongly indicates that the galaxy is undergoing a merger phase, leading to continual alterations in their appearance. We have also examined how the galaxy’s ellipticity and position angle change with its radius, as depicted in the upper-right panel of **Figure 3**. Notably, the galaxy appears nearly spherical towards its center, but as we move outward, it becomes more elliptical. This suggests that the outer regions of the galaxy are becoming more elongated, indicating a potential tidal connection and influence.

We used the Sérsic profile to model the galaxy’s surface brightness profile, as shown in the lower left panel of **Figure 3**. The Sérsic index for the fit, represented by “n”, is 0.8, and we measured an effective radius of 6.62 arcseconds. These values indicate that the galaxy has a relatively flat brightness distribution, resembling an exponential profile. This suggests that the distribution of stars is more spread out and less concentrated toward the center.

The Petrosian radius is a measure of the size of a galaxy, and it is derived from the Petrosian function, which helps in characterizing the overall extent of a galaxy’s light profile. It takes into account variations in a galaxy’s brightness, making it particularly useful for galaxies with diverse structures. The Petrosian index is a dimensionless profile that represents the rate of change of surface brightness with radius in a galaxy’s light profile. The Petrosian index is useful in determining radial concentrations of galaxy light profiles and performing accurate measurements of galaxy radii [33]. In our analysis, we calculated the Petrosian radius, specifically with a Sérsic index (n) of 0.2, which indicates how much light is distributed at different distances from the galaxy’s center.

At a distance of $2a_p$ (twice the Petrosian radius), we assume that the Petrosian profile encompasses the entirety of the galaxy’s brightness. This assumption allows us to effectively capture the overall extent of the galaxy’s light distribution seen in the lower right panel of **Figure 3**. Moreover, the half-light radius of the galaxy is estimated to be 2.73 arcsec.

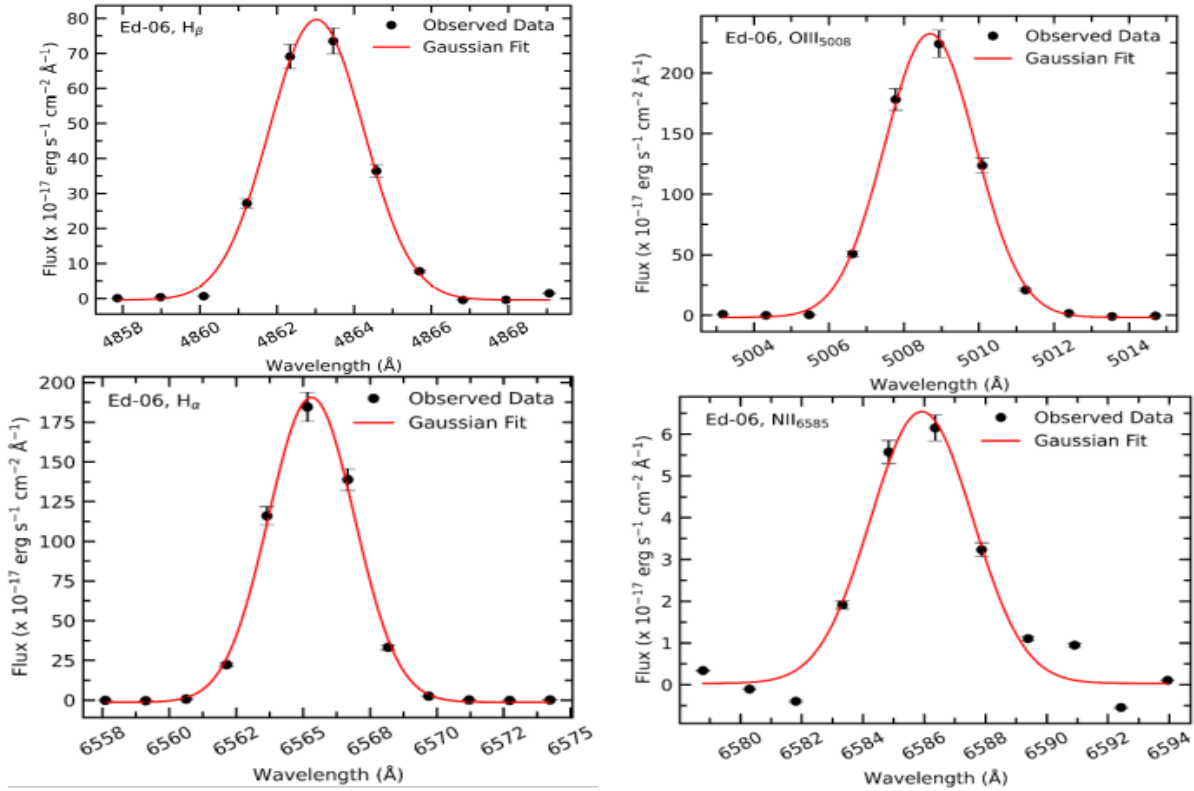


Figure 2: The figure illustrates the Gaussian profile of the galaxy’s prominent emitted spectral lines H_{β} , $OIII_{5008}$, H_{α} , and NII_{6585} . The error bars reflect the percentile error associated with the observations. We show a conservative estimate of the flux error in the plot, i.e., 10% of the observed flux provided by the SDSS webpage (<https://www.sdss.org/dr15/spectro/caveats/>). The wavelengths given in the X-axis are redshift corrected.

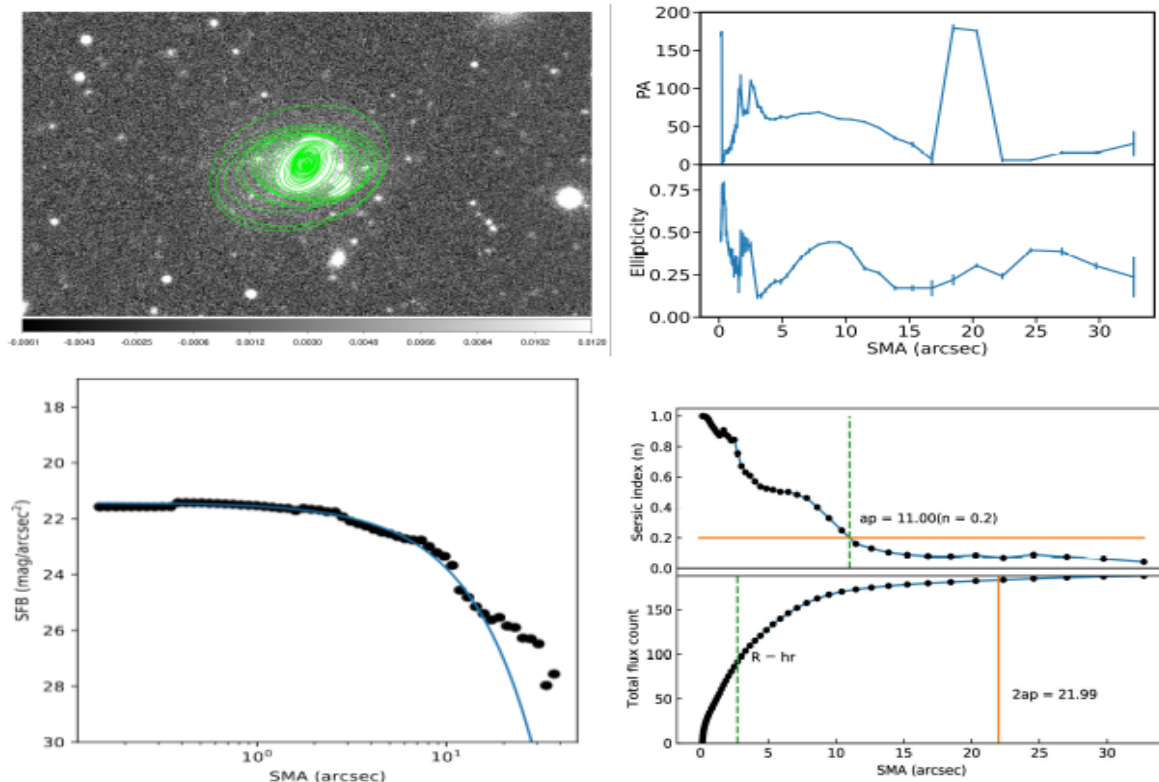


Figure 3: Caption of Figure 3 is given in next page.

Figure 3 (Caption): The upper left panel shows the isophotes of the interacting dwarf galaxy, Mrk 1481. The green ellipses represent the contour levels of the galaxy. The upper right panel shows the radial profile of position angle and ellipticity. The brightness profile of the galaxy is illustrated in the lower left panel, where the black dots represent the observed data and the blue solid line depicts the 1D Sérsic fitting of the galaxy. The lower right panel shows the radial profile of the Petrosian index and cumulative intensity at the g-band. The vertical dashed line represents the Petrosian radius at Sérsic index 0.2 (horizontal brown line). The vertical green-colored dashed line intersects the curve at a half-light radius.

4 Conclusion

In our comprehensive analysis of the spectroscopic and photometric attributes of the interacting dwarf galaxy, Mrk 1481, we made a noteworthy discovery. Our observations revealed the presence of highly prominent gas emission lines, indicating that the galaxy is currently undergoing a starburst phase, with the formation of very young stars in progress. To quantify this star formation activity, we conducted Gaussian profile fits of the emission lines and calculated the total flux, a key parameter in determining the galaxy's star formation rate. Our findings indicate a remarkably high star formation rate, measuring at $0.0046 \text{ M}_{\odot} \text{ yr}^{-1}$ when using the H_{α} lines. However, after applying an extinction correction, this rate increases to $0.0055 \text{ M}_{\odot} \text{ yr}^{-1}$. This adjustment underscores the active nature of star formation within the galaxy, highlighting the intensity of this ongoing process. We also calculated the metallicity of the galaxy which comes out 8.88 dex, and it shows that the galaxy is very metal-rich and young stars are forming. Additionally, we delved into the photometric characteristics of the galaxy. We employed a Sérsic profile to model the galaxy, with a Sérsic index of 0.8 and a half-light radius of 2.73 arcseconds. The analysis of changing ellipticity and position angle of the galaxy has led us to the observation that the galaxy is undergoing a merger, particularly at its outer regions, indicating a potential tidal connection and influence.

Acknowledgements

Daya Nidhi Chhatkuli acknowledges the University Grants Commission of Nepal, for financial support (Award No.: PhD-75/76-S & T-13) to carry out this research.

This study is based on the archival images and spectra from the Sloan Digital Sky Survey (<http://www.sdss.org/collaboration/credits.html>).

A Brief Statement on the Observational Data Sources

The Sloan Digital Sky Survey (SDSS) is a comprehensive astronomical survey that has played a pivotal role in mapping the night sky and gathering data on a vast number of celestial objects. Observations of celestial objects, including Mrk 1481,

often involve multiple telescopes and instruments across different wavelengths. We use SDSS data to study the spectra, photometry, and other characteristics of galaxies, quasars, and various celestial bodies. To understand Mrk 1481, we have used SDSS data to analyze its spectral features, measure its redshift, study its morphology, and derive information about its physical properties. The SDSS data is publicly accessible and has become an invaluable resource for astronomers worldwide. Its extensive databases, including images, spectra, and catalogs, support a wide range of astronomical research, from studying individual objects to investigating the large-scale structure of the cosmos. The SDSS web site is www.sdss.org.

References

- [1] J. S. Farnes. A unifying theory of dark energy and dark matter: Negative masses and matter creation within a modified Λ CDM framework. *Astronomy & Astrophysics*, 620:A92, 2018. <https://doi.org/10.1051/00046361/2018>
- [2] B. E. Robertson et al. Galaxy formation and evolution science in the era of the large synoptic survey telescope. *Nature Reviews Physics*, 1:450–462, 2019. <https://doi.org/10.1038/s42254-019-0067-x>
- [3] J. Salcido et al. The impact of dark energy on galaxy formation. what does the future of our universe hold? *Monthly Notices of the Royal Astronomical Society*, 477:3744–3759, 2018. <https://doi.org/10.1093/mnras/sty879>
- [4] S. L. Ellison et al. Galaxy mergers can rapidly shut down star formation. *Monthly Notices of the Royal Astronomical Society: Letters*, 517:L92–L96, 2022. <https://doi.org/10.1093/mnrasl/slac109>
- [5] T. Naab and J. P. Ostriker. Theoretical challenges in galaxy formation. *Annual Review of Astronomy and Astrophysics*, 55:59–109, 2017. <https://www.annualreviews.org/doi/10.1146/annurev-astro-081913-040019>
- [6] W. Pearson et al. Effect of galaxy mergers on star-formation rates. *Astronomy & Astro-*

- physics*, 631:A51, 2019. <https://doi.org/10.1051/0004-6361/201936337>
- [7] D. N. Chhatkuli et al. Forming blue compact dwarf galaxy through mergers. *Monthly Notices of the Royal Astronomical Society*, 520:4953–4960, 2023. <https://doi.org/10.1093/mnras/stac3700>
- [8] K. George and K. Zingade. Revealing the nature of star forming blue early-type galaxies at low redshift. *Astronomy & Astrophysics*, 583:A103, 2015. <https://doi.org/10.1051/0004-6361/201424826>
- [9] H.-X. Zhang et al. The blue compact dwarf galaxy vcc 848 formed by dwarf–dwarf merging: H i gas, star formation, and numerical simulations. *The Astrophysical Journal*, 900:152, 2020.
- [10] A. Barnes et al. Star formation rates and efficiencies in the galactic center. *Monthly Notices of the Royal Astronomical Society*, 469(2):2263–2285, 2017. <https://doi.org/10.1093/mnras/stx941>
- [11] R. Feldmann. The link between star formation and gas in nearby galaxies. *Communications Physics*, 3(1):226, 2020. <https://doi.org/10.1038/s42005-020-00493-0>
- [12] M. R. Krumholz. The big problems in star formation: The star formation rate, stellar clustering, and the initial mass function. *Physics Reports*, 539(2):49–134, 2014. <https://doi.org/10.48550/arXiv.1402.0867>
- [13] P. Weilbacher and U. Fritze-v. Alvensleben. On star formation rates in dwarf galaxies. *Astronomy & Astrophysics*, 373, 2001. <https://doi.org/10.1051/0004-6361:20010704>
- [14] R. Genzel et al. A study of the gas–star formation relation over cosmic time. *Monthly Notices of the Royal Astronomical Society*, 407:2091–2108, 2010. <https://doi.org/10.1111/j.1365-2966.2010.16969.x>
- [15] R. Genzel et al. The metallicity dependence of the $\text{CO} \rightarrow \text{H}_2$ conversion factor in $z \geq 1$ star-forming galaxies. *The Astrophysical Journal*, 746:69, 2012.
- [16] T. Jeřábková et al. Impact of metallicity and star formation rate on the time-dependent, galaxy-wide stellar initial mass function. *Astronomy & Astrophysics*, 620:A39, 2018. <https://doi.org/10.1051/0004-6361/201833055>
- [17] Y. Komiyama et al. A photometric and spectroscopic study of dwarf and giant galaxies in the coma cluster. i. wide-area photometric survey: Observation and data analysis. *The Astrophysical Journal Supplement Series*, 138:265, 2002. <https://doi.org/10.1086/324644>
- [18] J. M. Lotz et al. The evolution of galaxy mergers and morphology at $z < 1.2$ in the extended groth strip. *The Astrophysical Journal*, 672:177, 2008. <https://doi.org/10.1086/523659>
- [19] S. Courteau et al. The luminosity profile and structural parameters of the andromeda galaxy. *The Astrophysical Journal*, 739:20, 2011. <https://doi.org/10.1088/0004-637X/739/1/20>
- [20] S. Paudel et al. A catalog of merging dwarf galaxies in the local universe. *The Astrophysical Journal Supplement Series*, 237:36, 2018. <https://doi.org/10.3847/1538-4365/aad555>
- [21] R. C. Kennicutt Jr. The rate of star formation in normal disk galaxies. *Astrophysical Journal*, 272:54–67, 1983. <https://doi.org/10.1086/161261>
- [22] R. C. Kennicutt Jr. The star formation law in galactic disks. *The Astrophysical Journal*, 344:685–703, 1989. <https://doi.org/10.1086/167834>
- [23] R. I. Jedrzejewski. CCD surface photometry of elliptical galaxies–i. observations, reduction, and results. *Monthly Notices of the Royal Astronomical Society*, 226(4):747–768, 1987. <https://doi.org/10.1093/mnras/226.4.747>
- [24] J. L. Sersic. *Atlas de galaxias australes*. 1968.
- [25] A. Domínguez et al. Dust extinction from balmer decrements of star-forming galaxies at $0.75 \leq z \leq 1.5$ with hubble space telescope/wide-field-camera 3 spectroscopy from the WFC3 infrared spectroscopic parallel survey. *The Astrophysical Journal*, 763(2):145, 2013. <https://doi.org/10.1088/0004-637X/763/2/145>
- [26] B. Vulcani et al. Gasp. viii. capturing the birth of a tidal dwarf galaxy in a merging system at $z \sim 0.05$. *The Astrophysical Journal*, 850(2):163, 2017. <https://doi.org/10.3847/1538-4357/aa9652>
- [27] R. Leaman et al. Triggered star formation in a merging, gas-rich dwarf galaxy around ngc

7241. *Monthly Notices of the Royal Astronomical Society*, 450(3):2473–2485, 2015. <http://doi.org/10.1093/mnras/stv626>
- [28] D. N. Chhatkuli, S. Paudel, and B. Aryal. A detailed morphological and spectroscopic study of merging dwarf galaxy PGC 030133. *Journal of Nepal Physical Society*, 7(4):28–35, 2021. <http://doi.org/10.3126/jnphysoc.v7i4.42928>
- [29] Y. Zhao et al. The stellar population and star formation properties of blue compact dwarf galaxies. *The Astronomical Journal*, 141(2):68, 2011. <http://doi.org/10.1088/0004-6256/141/2/68>
- [30] D. Stern and H. Spinrad. Search techniques for distant galaxies. *Publications of the Astronomical Society of the Pacific*, 111(766):1475, 1999. <https://iopscience.iop.org/article/10.1086/316471/pdf>
- [31] C. Allende Prieto, D. L. Lambert, and M. Asplund. The forbidden abundance of oxygen in the sun. *The Astrophysical Journal Letters*, 556(1):L63–L66, 2001. <http://doi.org/10.1086/322874>
- [32] Y. Zhao, Y. Gao, and Q. Gu. Luminosity–metallicity relations for blue compact dwarf galaxies in the optical and near-infrared. *The Astrophysical Journal*, 710(1):663, 2010.
- [33] R. Geda, S. M. Crawford, L. Hunt, M. Bershadsky, E. Tollerud, and S. Randriamampandry. Petrofit: A python package for computing petrosian radii and fitting galaxy light profiles. *The Astronomical Journal*, 163(5):202, 2022. <https://doi.org/10.3847/1538-3881/ac5908>